

Effect of Carbon Content on Three-body Abrasive Wear Characteristics of 28Cr-3Ni Cast Alloys

Takayuki TODAKA, Kazumichi SHIMIZU, Kenta KUSUMOTO, Riki Hendra PURBA* and Yila GAQI

Muroran Institute of Technology, 27-1 Mizumoto, Muroran City, Hokkaido, 050-8585 Japan.

(Received on March 17, 2021; accepted on May 13, 2021)

Abrasive wear resistance of white cast iron can be improved by adding transition metals due to carbide formation and matrix stabilization. However, it must also be affected by carbon content which has received little attention from researchers. Therefore, this study would investigate the influence of (1.4 and 2.8 wt.%) C on three body abrasive wear characteristics of 28Cr-3Ni cast alloys. High Cr-based multi-component white cast irons (Hi-Cr MWCI) were used as comparison materials to estimate the life-service of each material. The abrasion test was performed using a rubber wheel abrasion machine test with two different sizes of silica sands (1100HV1).

As results, the microstructure consists of martensite (the main matrix) and M_7C_3 carbide. Additionally, M_2C carbide was also precipitated on the microstructure of Hi-Cr MWCI. Meanwhile, Ni or Co was embedded in the matrix area of materials microstructure. In the case of 28Cr-3Ni, the higher amount of C has a higher carbide volume fraction and hardness leading to be better abrasive wear resistance at high loads. However, the reverse trend occurred at low loads with different sizes of abrasive particles. By comparing to Hi-Cr MWCI, its abrasive wear resistance is lower owing to the fewer carbide types. In the case of Hi-Cr MWCI, the higher Cr addition significantly consumes C content during the solidification process resulting to lower hardness and wear resistance. Therefore, it can be concluded that the three abrasive wear performance of materials is strongly influenced by C content, applied load, and abrasive particle size.

KEY WORDS: carbon; high chromium; multicomponent white cast iron; abrasive wear.

1. Introduction

According to ASTM, the definition of abrasive wear can be described as progressive material loss due to hard protuberance is pressed and moved along the material surface. It can be accoutered in wide-range mechanical parts or fields such as dump truck buckets, crushers, agricultural equipment, rolling mills, pulverizing, *etc.* This abrasive wear phenomenon can spend 1–4% of gross national product as estimated in the previous research. Therefore, there is a great demand for exceptional abrasive wear-resistant materials.^{1,2)}

The elements of Chromium (Cr) and carbon (C) can form carbide during the solidification process on Fe–Cr–C system which provides better abrasive wear resistance. There are several kinds of chromium carbide such as M_3C , M_7C_3 , $M_{23}C_6$, *etc.* where the more addition of Cr will have a higher carbide volume fraction (CVF).^{3–5)} In most studies, it has been revealed that the high chromium white cast iron (HCCI) containing M_7C_3 carbide is more resistant to abrasive wear than other carbide types due to its higher

hardness. However, at the same time, it is easy to crack due to low toughness resulting in limited application.^{6–14)} Many attempts have been made by scholars to obtain a higher abrasive wear resistance of HCCI without scarifying its toughness by reducing the size of the M_7C_3 carbide. It has been known that the better wear resistance of HCCI can be achieved by adding stronger carbide forming elements such as Ti, Nb, *etc.* It can be understood that the Ti or Nb will firstly consume carbon in the melt to form TiC or NbC carbides, then, when the melt reaches the precipitation temperature of M_7C_3 carbide, the smaller M_7C_3 carbide will be dissolved on the microstructure leading to better abrasive wear resistance.^{15–18)} Another effort, plural carbide forming elements (Cr, Mo, W, and V) have been added simultaneously into white cast iron, namely multi-component white cast iron (MWCI) for certain cases such as rolling mills, pulverizing, *etc.* in recent decades. It is known that the more variety of carbides formed in the microstructure results in higher hardness and wear resistance.^{19–21)} Besides that, it has been developed in earlier work by adding Ni (range: 0–5 wt.%) into MWCI. It has been clearly explained that Ni will not act as a carbide forming element but preferentially dissolve in the matrix of material and encourage the carbide

* Corresponding author: E-mail: 20096010@mmm.muroran-it.ac.jp



formation leading to be better wear resistance at elevated temperatures. However, although it produces more carbide, it can significantly reduce the hardness of the material if the addition exceeds 3 wt.% at room temperature.²²⁾

The abrasive wear resistance of HCCI can also be improved by modifying the matrix through the destabilization heat-treatment process. It has been a long time known that HCCI with martensite matrix is higher abrasive wear resistance than austenite or ferrite and pearlite. In addition, the precipitation of secondary carbide will occur during the hardening process which contributes positively to abrasive wear resistance by reinforcing the matrix of HCCI. The heat treatment process depends on the chemical composition of the material itself.^{23–26)}

However, when the above transition metals are added to HCCI, super high-cost production is unavoidable. In addition, most of the published papers only emphasize the effect of transition metals, whereas the microstructure constituents (carbide and matrix) and abrasive wear performance are also strongly influenced by the C content. Indeed, in the case of HCCI, it has been known that the hypo-eutectic shows better wear resistance compared to hyper-eutectic.^{27,28)} However, the study about the influence of C in hypo-eutectic with Ni addition is still rarely investigated leading to poor explanations. Based on these reasons, the present work aims to systematically investigate the influence of C addition (1.4–2.8 wt.%) on three-body abrasive wear characteristics of 28Cr-3Ni cast alloys. In addition, it will be compared to high-Cr MWCI to estimate their life service.

2. Methodology

2.1. Material Preparation

In this present work, it was added 1.4 and 2.8 wt.% C into 28Cr-3Ni cast alloys. Briefly, the manufacturing steps can be highlighted as firstly 50 kg of raw materials were melted using high induction furnace and poured into Y sand block mold. Then, the Y- ingot was cut with 50 mm × 10 mm × 10 mm (see Fig. 1). Each specimen was heated to 1 323 K for two hours then cooled to room temperature by air cooling. Then, it was continued to tempering the process at 723 K for two hours to reduce the excessive retained austenite. As earlier described, it would be compared to 18 and 27 wt.% Cr based 3 wt.% (V, Mo, W, and Co) to estimate the life-service of materials. Since it would be added high Cr and some strong carbide forming elements into both high Cr based MWCI, it might produce high hardness and low toughness materials. Base on previous studies,^{29,30)} the toughness of material should be also considered in wear application by maintaining the amount of retained austenite. Therefore, both materials would be only

quenched without tempering (at 1 273 K and 1 323 K for 18Cr MWCI and 27Cr MWCI, respectively) to maintain the existence of retained austenite in the microstructure. The heat treatment temperatures were chosen because in this condition each material has the highest hardness due to matrix transformation and secondary carbide precipitation.^{31,32)} However, further research can be conducted on the effect of heat-treatment temperature on abrasive wear conditions. The chemical composition of alloys was measured using SPECTROLAB (AMATEK, Inc. America) as described in Table 1. It was used Optical Microscope (OM) and Scanning Electron Microscopy (SEM and EDS with type JXA-9800 R, Japan) to investigate the microstructure of each specimen. Before analyzing the microstructure, the specimens were etched in 5% nitro hydrochloric acid for several minutes. In addition, ImageJ as an engineering software supported SEM image was utilized to calculate the carbide volume fraction (CVF). It was used a grinder machine to clean each material surface after heat treatment (GS52PF, Kuroda Seiko Co., Ltd).

2.2. Three-body Abrasive Wear Testing

It was used a rubber wheel three-body abrasive wear machine according to ASTM G65 to evaluate the abrasion characteristic of each material as shown in Fig. 2(a). There were three different applied load numbers; 73.5, 147, and 196 N. The specimens would firstly be placed at the test piece holder and the machine test was set at 100 rpm for 360 s before the testing. It was used about 2.5 kg particle in every test which was poured into sand supply hopper. During the experiment, the abrasive particle would be automatically poured and against the surface of the targeted material. The wear rate of material was calculated by dividing weight material loss with distance as written on the following equation:

$$\text{Wear rate} = \frac{\Delta m}{\pi d t n} \dots\dots\dots (1)$$

Where Δm is material weight loss; d is the diameter of the wheel; t is time; n is rotating speed.

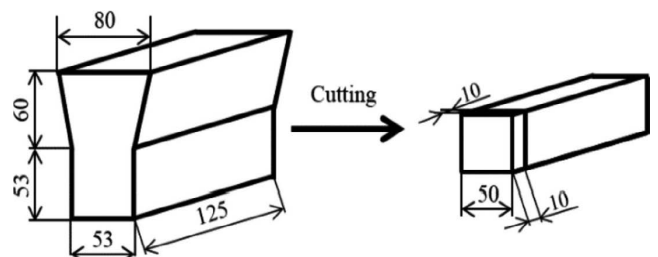


Fig. 1. The process of making specimens from Y- block.

Table 1. Chemical compositions of specimens (wt.%).

Specimen	C	Cr	Mo	V	W	Ni	Co	Mn	Si	P	Fe
1.4C-28Cr-3Ni	1.33	27.49	–	–	–	3.20	–	0.62	1.32	0.02	Bal.
2.8C-28Cr-3Ni	2.56	27.32	–	–	–	3.23	–	0.59	1.41	0.03	Bal.
18Cr-MWCI	3.03	15.88	2.59	2.74	2.68	–	2.70	0.21	1.39	0.02	Bal.
27Cr-MWCI	2.83	27.13	2.63	2.98	2.72	–	2.69	0.19	0.98	0.02	Bal.

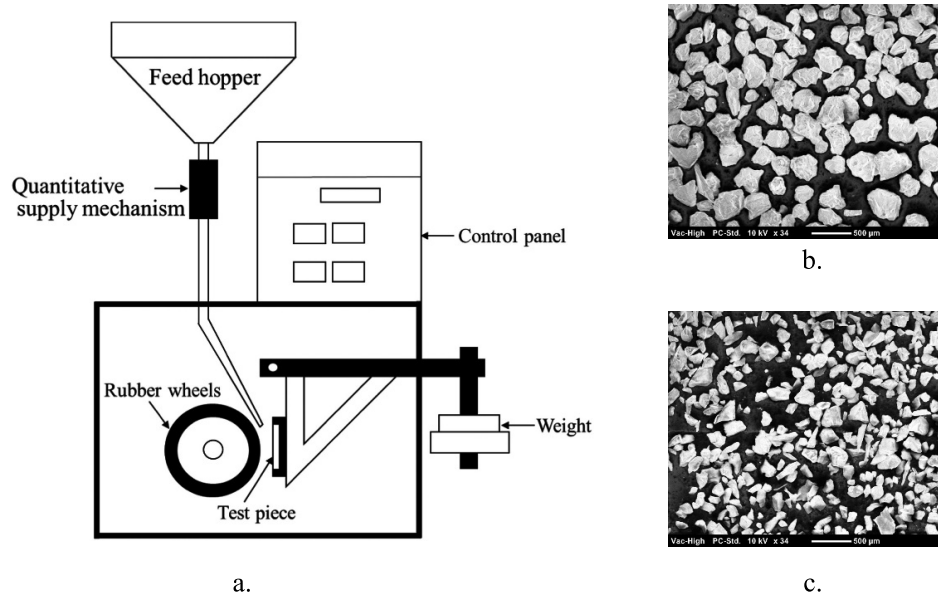


Fig. 2. a. Outline of the rubber wheels three abrasive wear machine test; b. and c. are abrasive particles number 6 and 8, respectively.

Also, it was analyzed the influence of silica sand size as an abrasive particle rather than only the number of applied loads. The average size of particles is $300\ \mu\text{m}$ for sand number 6 (Fig. 2(b)) and $75\ \mu\text{m}$ for sand number 8 (Fig. 2(c)) with 1100HV1 hardness.

2.3. Vickers Hardness Test

Initially, each material was cut with a dimension of $10\ \text{mm} \times 10\ \text{mm} \times 10\ \text{mm}$ and polished. Then, the micro and macro hardness were measured using The Future-Tech Co. Ltd.: FV-800 and the Future-Tech Co. Ltd.: FM-300. The macro-hardness indicates as entirely material hardness (matrix plus carbide), while micro-hardness is matrix only.

3. Result and Discussion

3.1. Hardness of Material

The hardness of material usually plays an important factor in abrasive wear characteristic of HCCI even though its toughness is also worthily considered.¹⁰⁻¹² Therefore, the hardness of the present alloys was measured with 14 times repetition test as depicted in Fig. 3 and the error bar is as standard deviation. As previously mentioned, there are two kinds of measured hardness in this study. They are macro-hardness that indicates overall specimens' hardness (matrix and carbide) and micro-hardness is matrix only.

The result shows that the micro and macro hardness of 1.4C-28Cr-3Ni are $323.24 \pm 16.16\text{HV}0.1$ and $437.47 \pm 21.88\text{HV}30$. Meanwhile, it is $438.24 \pm 21.91\text{HV}0.1$ and $626.11 \pm 31.30\text{HV}30$ in the case of 2.8C-28Cr-3Ni, respectively. It reveals that either micro- or macro- hardness is increased significantly by increasing the amount of C addition as expected. However, even though 2.8C-28Cr-3Ni has a higher hardness value, it is lower than both high Cr MWCI. It can be presumed owing to the more carbide types precipitated in the microstructure of both high Cr-MWCI during the solidification process and the different heat-treatment processes. The micro and macro hardness of 18Cr MWCI are $719.18 \pm 32.96\text{HV}0.1$ and $981.08 \pm 49.05\text{HV}30$, while, 27Cr

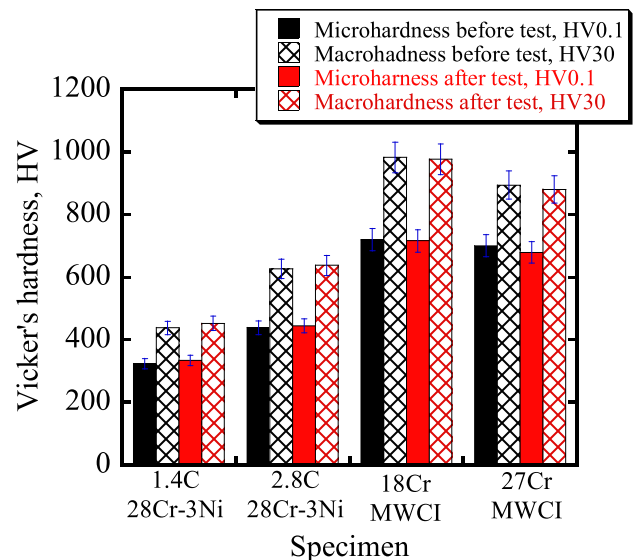


Fig. 3. Vickers hardness values of each material. (Online version in color.)

MWCI has $698.95 \pm 30.94\text{HV}0.1$ and $894.50 \pm 44.7\text{HV}30$, respectively. Generally, the higher amount of Cr addition will produce more carbides in the microstructure leading to be harder white cast iron.^{5,14} However, it does not relate to both high Cr MWCI which 18Cr MWCI has higher micro and macro-hardness than 27Cr MWCI. To determine the reason for this fact, it would investigate the microstructure of specimens in the further section. In addition, it can be seen that there is no significant difference in hardness after and before the test. This fact indicates no significant effect of the strain-induced transformation of retained austenite to martensite during the abrasive wear test.

3.2. Microstructure Evaluation

Generally, the microstructure constituents also contribute some important factors to abrasive wear conditions. Therefore, it was evaluated in the current issue. By using Optical Microscope (OM), it can be seen that the microstructure of

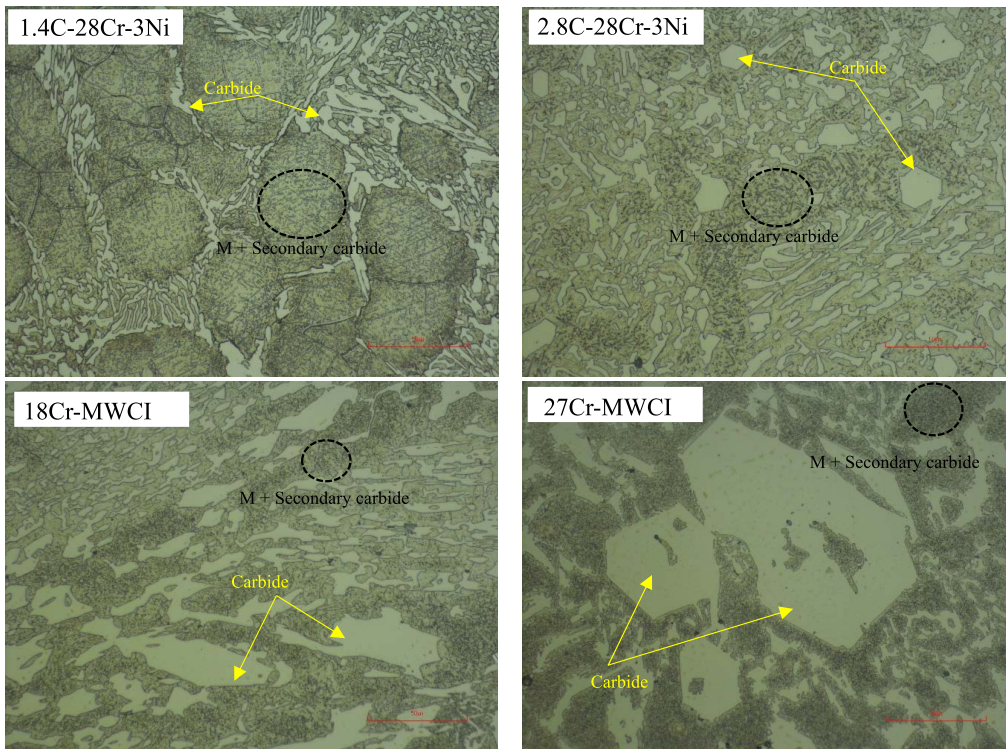


Fig. 4. Observation of material's microstructure using an Optical Microscope (OM). (Online version in color.)

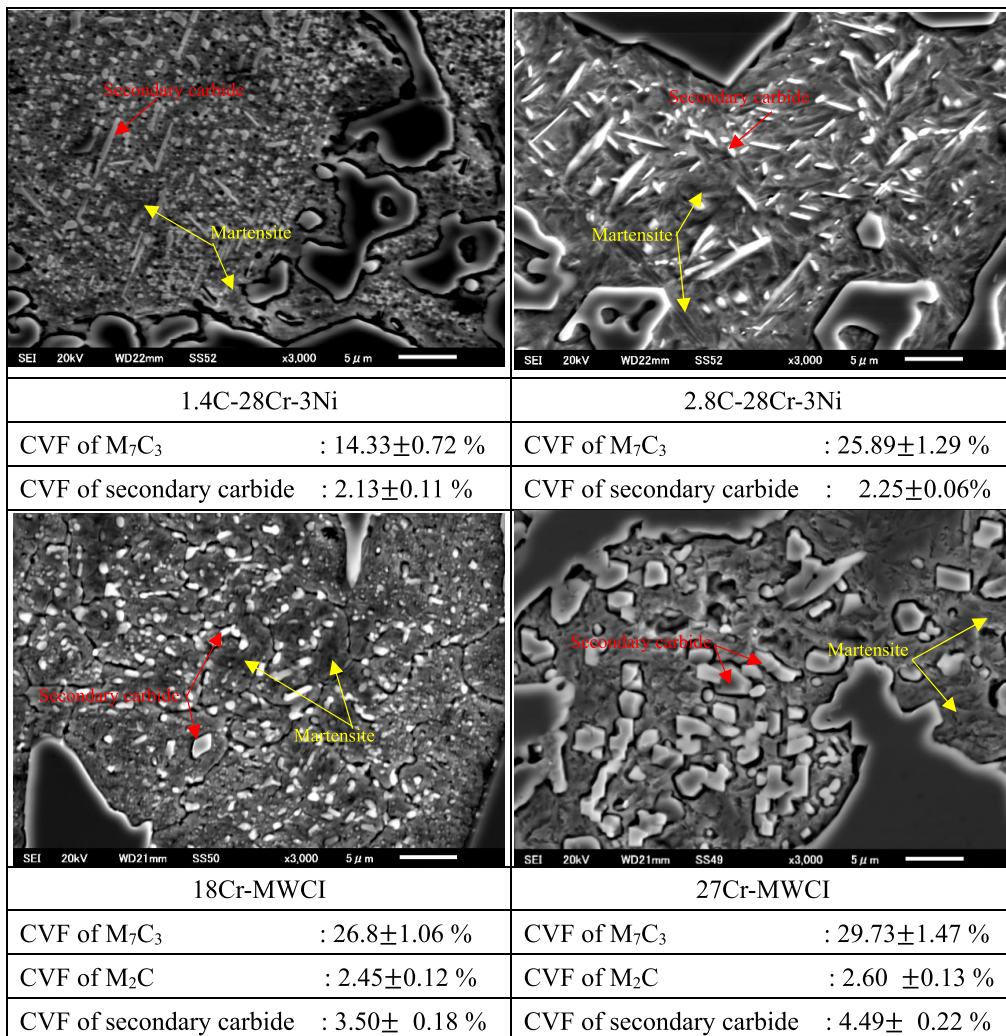


Fig. 5. Microphotograph of matrix and secondary carbide by using SEM and carbide volume fraction (CVF) of each material. (Online version in color.)

each material consists of the matrix and carbide as displayed in Fig. 4. The carbide is evenly dispersed except 1.4C-28Cr-3Ni. Primary carbide which has a hexagonal rod-like shape can be encountered on the microstructure of 2.8C-28Cr-3Ni and both high Cr MWCI. In higher magnification SEM (see Fig. 5), there are plenty of secondary carbides embedded in the matrix area. In the case of (1.4 and 2.8) C-28Cr-3Ni, the shapes of this secondary carbide are globular and fiber-like. Meanwhile, it is only globular in the case of (18 and 27) Cr

MWCIs which becomes coarser as increase the amount of Cr addition. The different shapes of the secondary carbide must be caused by different chemical compositions and heat-treatment steps. Additionally, it can be seen that the matrix of each material seems needle-like. By combination this image with microhardness and XRD data, it is inferred that martensite or bainite (300–900 HV)³³ is the main matrix type as an effect of the destabilization heat-treatment process. While the precipitation of each carbide as indexed by XRD (see Fig. 6) is caused by the high-affinity characteristic of C for Fe, Cr, and other transition metals.

The volume fraction of carbide was measured using binarizing image analysis as an engineering software and ImageJ on five randomly SEM microphotographs (see Fig. 5). It was found that the CVF of M_7C_3 was increased as increased the amount of C in the case of (1.4 and 2.8) C-28Cr-3Ni. This increment also occurs on both high Cr MWCI that was attributed by improving the amount of Cr. However, a significant improvement of secondary carbide was not observed. Therefore, the effect of secondary carbide could be ignored during wear investigation. The CVF of M_2C was not different on both high Cr MWCI that must be caused by the same amount of Mo and W addition. From this result, it can be said that the transition metals will bond the adjacent C in the iron melt to form carbide during the solidification process. It means the higher amount of its addition will require more concentration of C to form higher CVF. However, at the same time, the solubility of the C element in the matrix must decrease leading to softening. This condition can be proven by lowering the microhard-

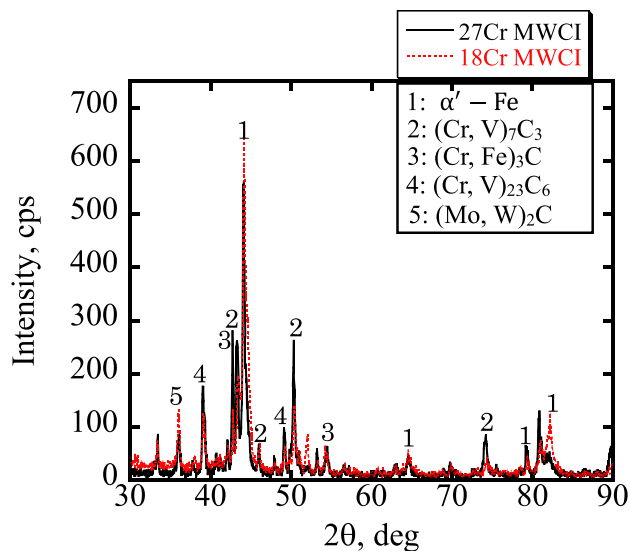


Fig. 6. X-ray diffraction of high chromium MWCI as representative materials. (Online version in color.)

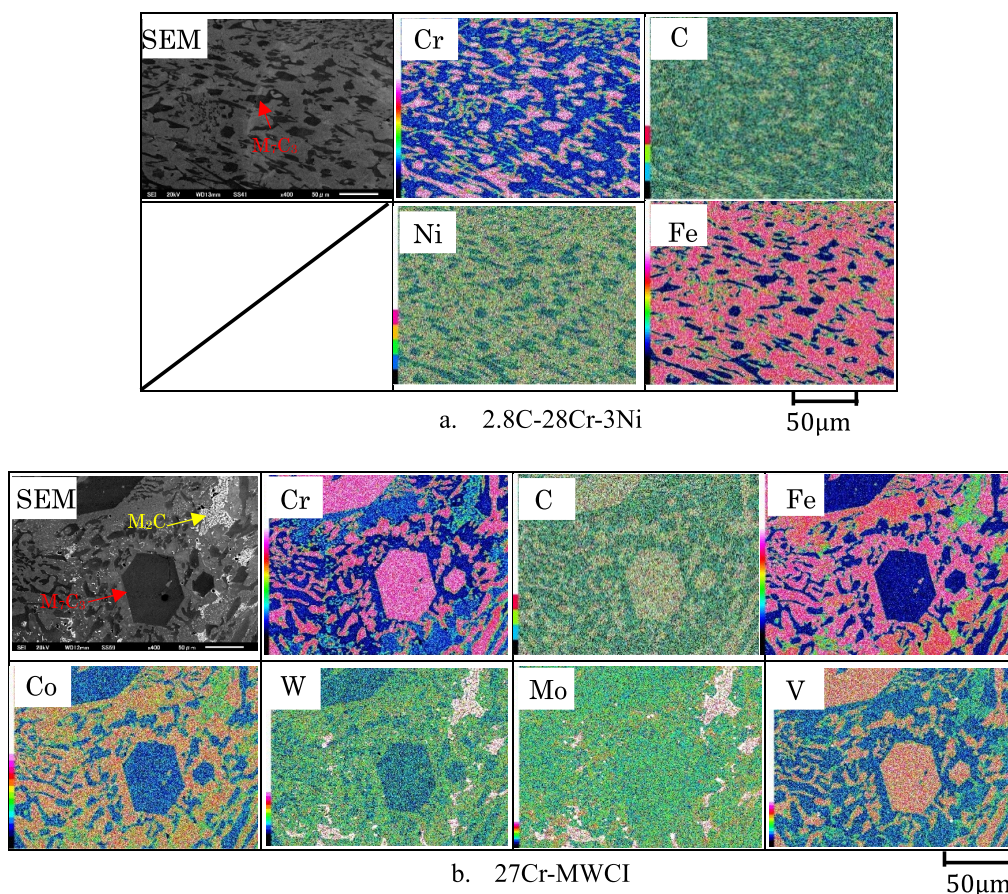


Fig. 7. SEM-EDS elemental mapping of representative material. (Online version in color.)

ness of 27Cr MWCI compared to 18Cr MWCI. Actually, through the carbon balance (C_{balance}) formula as an approach technique, it can estimate the solubility of C in the matrix of multi-component white cast iron in which the M_7C_3 carbide dissolves in the microstructure.^{36,37} The formula is written as the following:

$$C_{\text{balance}} = \%C \text{ in the cast iron} - \%C_{\text{stoich}}$$

$$\%C_{\text{stoich}} = 0.099(\%Cr) + 0.063(\%Mo) + 0.033(\%W) + 0.235(\%V).$$

It can be known that the C concentration in the matrix of 18Cr MWCI is about 0.22 while 27Cr MWCI has negative 0.67. Through this formula, it can be understood that despite the volume fraction of carbide increase or its size is getting bigger as increasing the amount of Cr, it will minimize the solubility of C in the matrix. Consequently, it will produce lower material hardness.

The EDS mapping (see Fig. 7) shows the distribution of each element on the microstructure. It can be seen that Ni and Co were embedded in the matrix with Fe which is in good agreement with the previous study. The Mo and W were dissolved in the same type of carbide as M_2C fishbone-like. Unlike some earlier studies,^{22,34} the V and C elements were not dissolved as V_2C , V_4C_3 , V_6C_6 , V_8C_7 , or VC carbide while it was completely embedded in the M_7C_3 area which relates to the XRD data. This different finding can be understood that the C element was mostly consumed by the Cr element during the solidification process due to higher addition than V. Therefore, it can be said that even though the V has larger negative mixing enthalpy ($\Delta H_{\text{mix}}V-C = -46.09$ kJ/mole) than Cr ($\Delta H_{\text{mix}}Cr-C = -14.98$ kJ/mole),³⁵ but, the amount of each transition metal also plays an important factor to form the carbide. Since the V is embedded simultaneously with Cr and C, the primary M_7C_3 carbide of 18Cr MWCI (about 54 μm) or 27Cr MWCI (about 86 μm) is larger compared to 2.8Cr-28Cr-3Ni (about 35 μm).

3.3. Three-body Abrasive Wear Behavior

The abrasive wear rate of each material at different num-

ber of applied loads is shown in Fig. 8(a) which has been obtained from three repetitions of the test. Overall, the material has the same tendency in which the higher number of applied load is the higher abrasive wear rate. The abrasive wear rate of 1.4C-28Cr-3Ni is significantly increased as increasing the load either using sand number 6 or 8 which is about 5.02×10^{-4} g/m and 1.7×10^{-4} g/m, respectively. While the wear rate is not sharply increased in the case of 2.8C-28Cr-3Ni owing to evenly distributed carbide and higher CVF which effectively covers the matrix from abrasive against. The highest abrasive wear rates are about 1.08×10^{-4} g/m and 0.68×10^{-4} g/m for sand numbers 6 and 8, respectively. When comparing both of them, the abrasive wear resistance of 1.4C-28Cr-3Ni is lower than 2.8C-28Cr-3Ni either using sand number 6 or 8 at a high load. This significant improvement must be influenced by the hardness of materials. However, it is interesting to see that at the lowest load, the hardness of the material is not consistent with abrasive wear resistance when using different sizes of silica sand. In which the abrasive wear rate of 1.4C-28Cr-3Ni with sand number 8 is lower than 2.8C-28Cr-3Ni using number 6. The reason for this fact would be explained in the next section. Figure 8(b) shows the abrasive wear behavior as a function of wheel rotation. All of the material experienced the same tendency which material loss would increase at the higher number of wheel cycles. However, there is no significant difference between 1.4C-28Cr-3Ni using sand number 8 and 2.8C-28Cr-3Ni using the sand number 8 or even number 6. Therefore, the size of the particle should be considered in the three-body abrasive wear characteristics rather than only involves the hardness of material at low load and number of wheel cycles.

The abrasive performance of (1.4 and 2.8) C-28Cr-3Ni would be compared to both high Cr MWCI on the highest number of applied load and cycle to get closer data with the real estimation of materials life-service. The result has been depicted in Fig. 9. It was found that the abrasive wear rates of 18Cr MWCI are about 0.51×10^{-4} g/m and 0.24×10^{-4} g/m for sand numbers 6 and 8, respectively. Meanwhile, it is about 0.51×10^{-4} g/m and 0.24×10^{-4} g/m

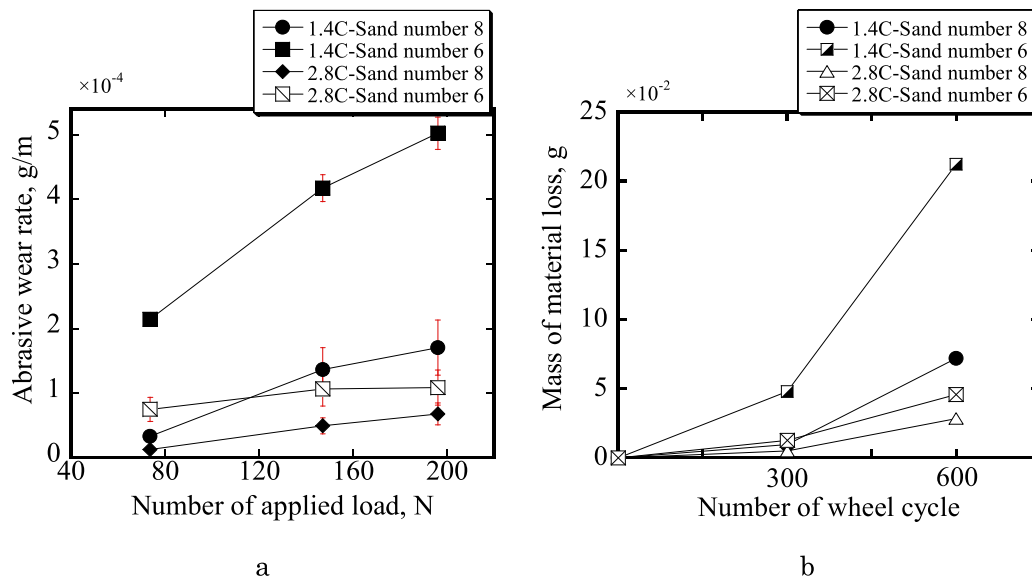


Fig. 8. a. wear rate of materials as function of applied loads; b. mass material loss vs cycles. (Online version in color.)

respectively in the case of 27Cr MWCI. The abrasive wear rate of 1.4C-28Cr-3Ni either using sand number 8 or 6 is very high compared to other materials which are associated with too low hardness and CVF, and different heat-treatment processes. The abrasive wear resistance of 2.8C-28Cr-3Ni is lower two times compared to 18Cr-MWCI and it is only about 20–30% difference to 27Cr MWCI. It reveals that the more various and amount of carbide forming elements is good to improve the abrasive wear resistance of high chromium white cast iron (HCCI). However, once it is added

over the threshold, the reverse result will occur since C is significantly bonded to form more CVF resulting in lowering matrix hardness and abrasive wear resistance of the material itself. It can be clearly stated that the solubility of C in the matrix is vital to be considered in the three-body abrasive wear condition.

3.4. Abrasive Wear Mechanism

To get a more detailed explanation of the three-body abrasive wear performance of each material, it would be observed the worn surface and cross-section after the test. **Figure 10** shows the worn surface of each material after the experiment using sand number 6 at 600 cycles and 196N. It can be seen the existence of groove which indicates the abrasive wear track on all of the material surfaces. Besides that, the pitting can be also encountered due to high hardness except for 1.4C-28Cr-3Ni. With a higher magnification of SEM as displayed on the right upper corner of Fig. 10, the appearance of micro-cutting can be observed on all of the worn surfaces which the clearer one belongs to 1.4C-28Cr-3Ni. This micro-cutting must be caused by the higher hardness value of abrasive particles (1100HV1) compared to specimens. In addition, the pitting can more clearly be observed on the M_7C_3 carbide area. From this point of view, it can be said the 1.4C-28Cr-3Ni has experienced micro-cutting as the main abrasive wear mechanism while the pitting phenomenon is also involved in others.

The material surface after the three-body abrasive wear test can be plotted using laser tech equipment as shown in **Fig. 11**. It can be seen the “shark teeth traces” which indicates the depth of abraded surface. The sharp down line as a circle with a red-dashed line denotes the micro-cutting mechanism. The topography gives the depth of the most

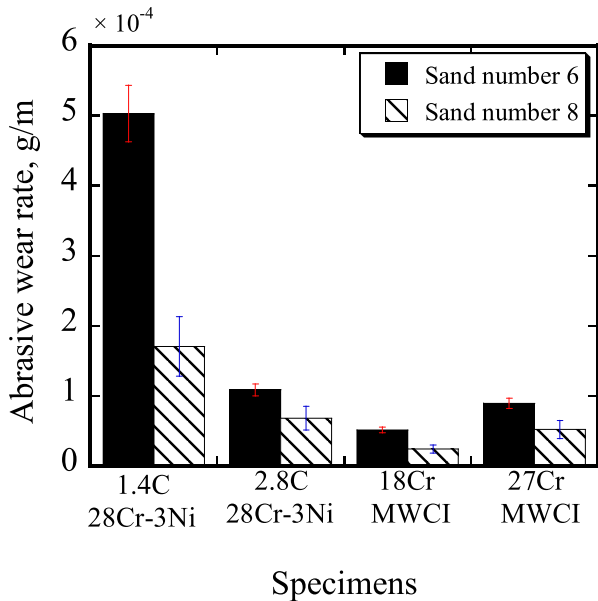


Fig. 9. Comparison abrasive wear rate of each material at 600 cycles with 196 N loads. (Online version in color.)

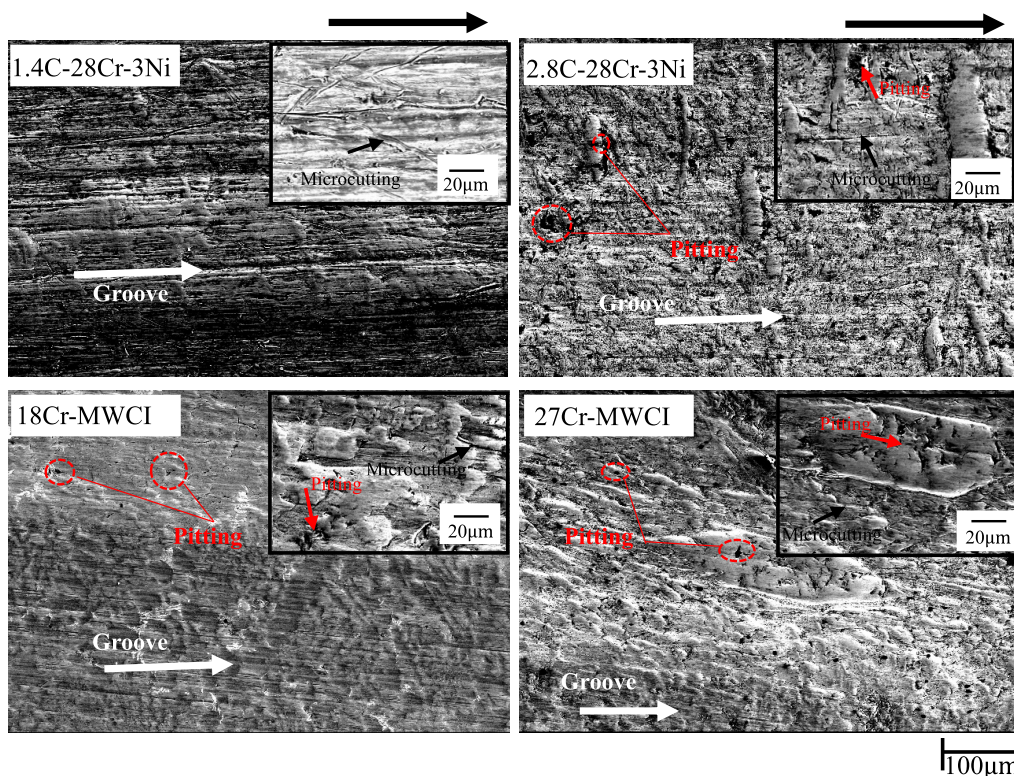


Fig. 10. SEM microphotograph of worn material surface after testing at 600 cycles with 196 N loads - sand number 6. (Online version in color.)

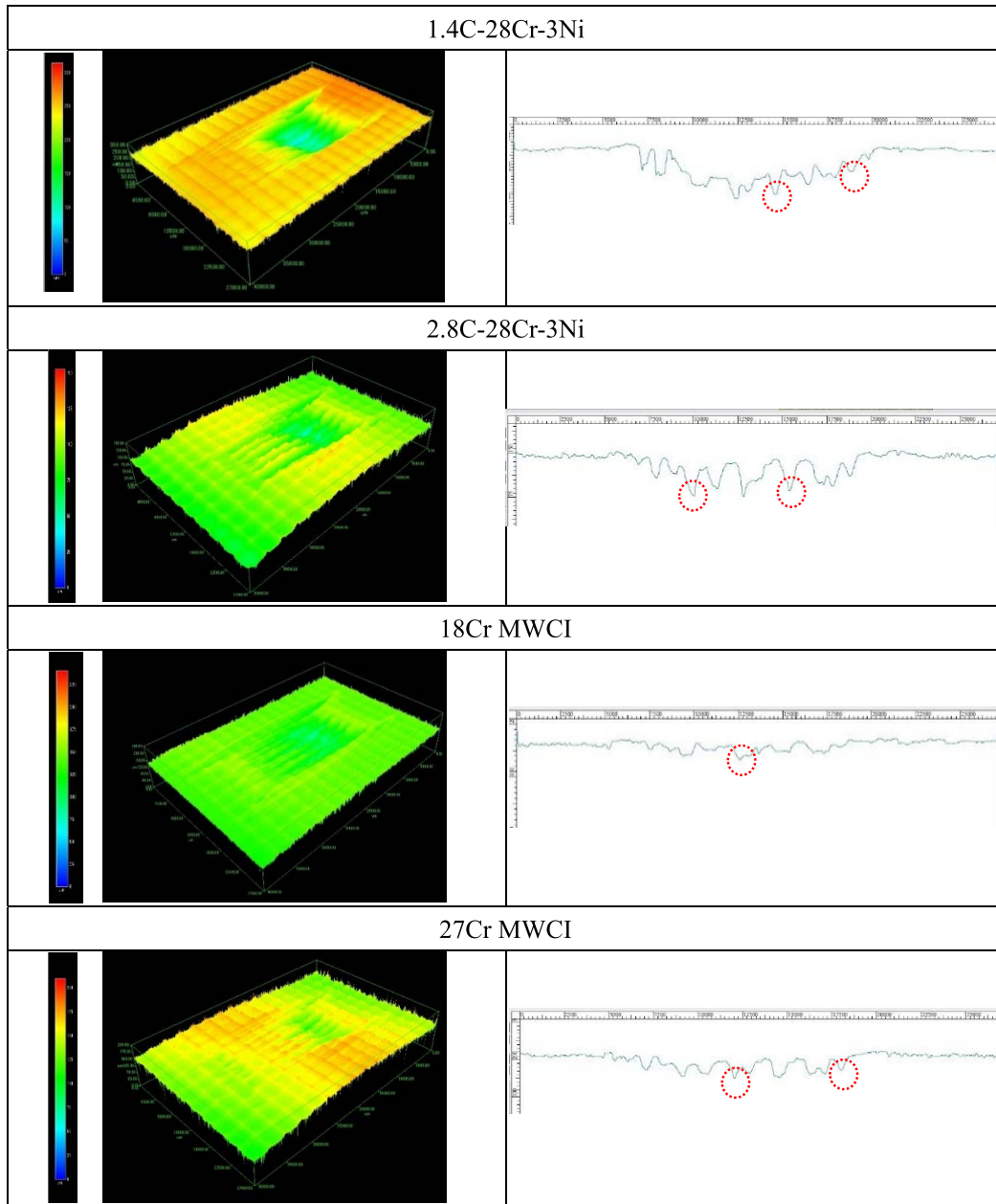


Fig. 11. Topographic observations of worn material surfaces using laser tech. (Online version in color.)

worn surface of each material as illustrated in Fig. 12. It reveals that the worn surface of 1.4C-28Cr-3Ni is deepest than others on both sand numbers which the shallowest belongs to 18Cr-MWCI. This result relates with the performance of each material that the deepest worn material surface indicates as the lowest abrasive wear resistance material.

Figure 13 shows the cross-section of the most abraded material surface at low load. It can be seen that the bigger particle size would make the severer matrix and carbide cracking. And, the higher amount of C shows the smoother one with the same sand number. However, it is interesting to see that the 1.4C-28Cr-3Ni/sand number 8 shows a better condition than 2.8C-28Cr-3Ni/sand number 6. It can be understood that the smaller sand would scrap the matrix and slip away the carbide leading to little damage and form the shadow zone on the matrix behind the carbide. Once the big sand abraded material's surface the bigger cracked car-

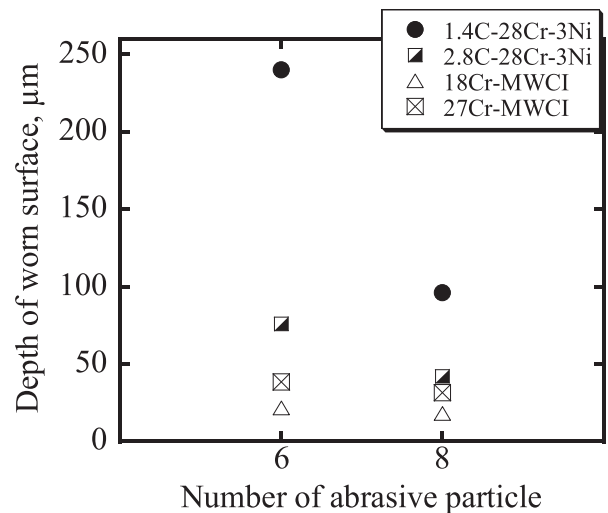


Fig. 12. The depth of material worn surface at 600 cycles with 196 N loads.

bide would directly peel out and no shadow zone observed. **Figure 14** has been drawn to simplify the explanation of this phenomenon. Therefore, at low load, the 1.4C-28Cr-3Ni is the better wear resistance using sand number 8 than 2.8C-28Cr-3Ni using sand number 6. Whilst, the different result occurred at the highest load (see **Fig. 15**) which is the worst condition belongs to the lower amount of C. However, 2.8C-28Cr-3Ni has a severer cross-section compared to both high Cr MWCI which must be caused by the lower CVF and fewer carbide types. It also shows that the matrix of 27Cr MWCI experienced the severer damage than 18Cr MWCI that must be attributed to the lower microhardness value. All of these findings are in accordance with the abrasive wear rate of each material. From this point of view, it can be emphasized that the three-body abrasive wear performance of each material is highly dependent on microstructure constituent, load, and sand size.

4. Conclusion

The effect of C on three-body abrasive wear characteristics of 28Cr-3Ni cast alloy has been investigated systematically in this current issue. Two high Cr MWCI have been utilized as comparable material to estimate the life-service of each material. All of the findings can be summarized as:

- (1) Higher C content can increase the CVF and hardness of 28Cr-3Ni cast alloys providing a better abrasive wear resistance at high load.
- (2) At low loads, the abrasive wear resistance is strongly influenced by the particle size in which the bigger size is the higher abrasive wear rate even though it has higher C addition.
- (3) The wear resistance is improved by various types of carbide element forming.
- (4) The concentration of C in the matrix is very important in the case of both high Cr MWCI.
- (5) The micro-cutting and pitting are the main abrasive

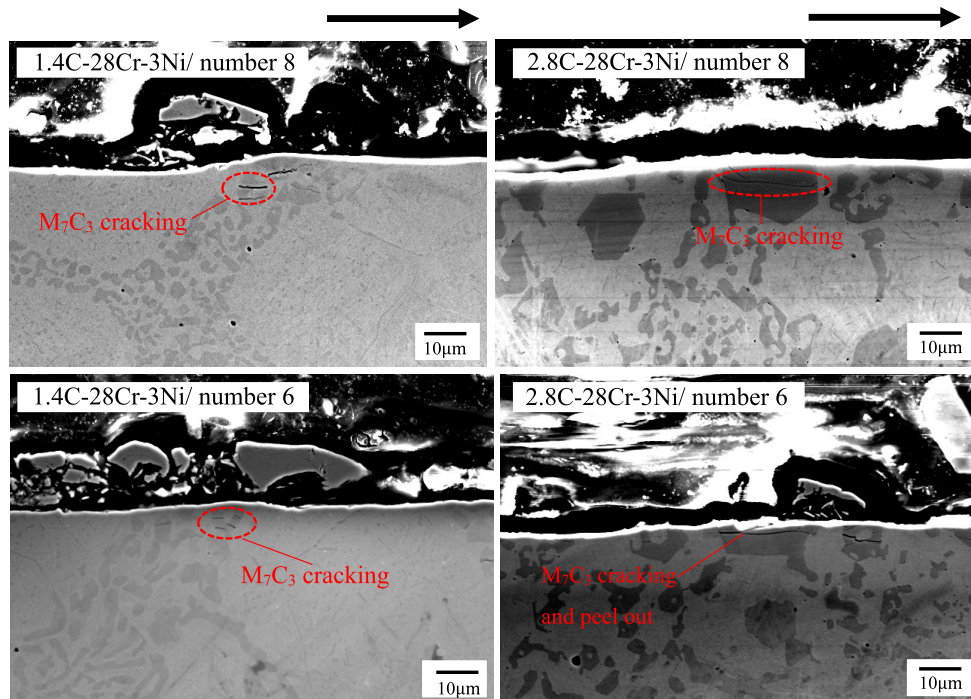


Fig. 13. Cross-section microphotograph of the most abraded surface after testing at 600 cycles with 73.5 N. (Online version in color.)

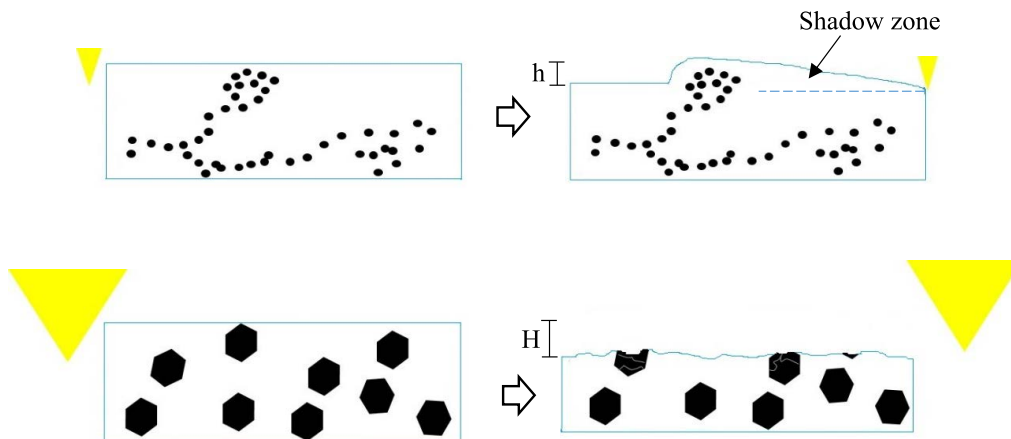


Fig. 14. Schematic cross-section depend on particles size at low load. (Online version in color.)

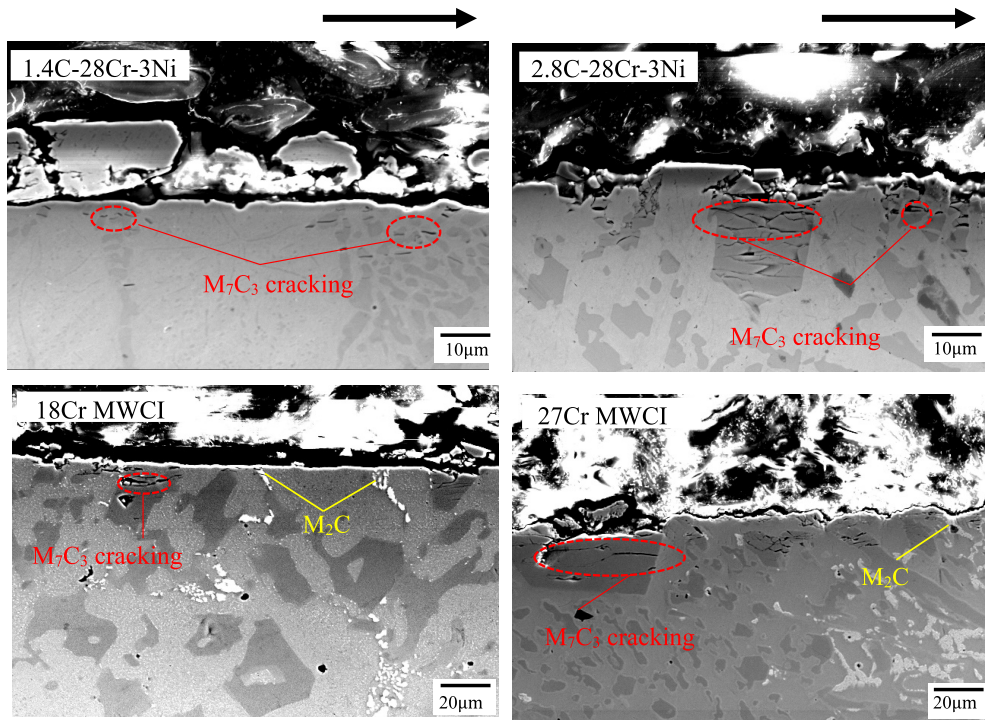


Fig. 15. Cross-section microphotograph of the most abraded surface after testing at 600 cycles with 196 N load - sand number 6. (Online version in color.)

wear mechanisms, except 1.4C-28Cr-3Ni.

REFERENCES

- 1) K. Holmberg and A. Erdemir: *Friction*, **5** (2017), 263. <https://doi.org/10.1007/s40544-017-0183-5>
- 2) T. Mang, K. Bobzin and T. Bartels: *Industrial Tribology: Tribosystems, Friction, Wear and Surface Engineering, Lubrication*, Wiley-VCH, Weinheim, (2011), 1.
- 3) C. P. Tabrett and I. R. Sare: *Scr. Mater.*, **38** (1998), 1747. [https://doi.org/10.1016/S1359-6462\(98\)00118-3](https://doi.org/10.1016/S1359-6462(98)00118-3)
- 4) E. Zumelzu, I. Goyos, C. Cabezas, O. Opitz and A. Parada: *J. Mater. Process. Technol.*, **128** (2002), 250. [https://doi.org/10.1016/S0924-0136\(02\)00458-2](https://doi.org/10.1016/S0924-0136(02)00458-2)
- 5) K. Shimizu, R. H. Purba, K. Kusumoto, X. Yaer, J. Ito, H. Kasuga and Y. Gaqi: *Wear*, **426–427** (2019), 420. <https://doi.org/10.1016/j.wear.2019.01.043>
- 6) Ö. N. Doğan, J. A. Hawk and G. Laird II: *Metall. Mater. Trans. A*, **28** (1997), 1315.
- 7) T. Sun, R. B. Song, X. Wang, P. Deng and C. J. Wu: *J. Iron Steel Res. Int.*, **22** (2015), 84.
- 8) E. Cortés-Carrillo, A. Bedolla-Jacuinde, I. Mejía, C. M. Zepeda, J. Zuno-Silva and F. V. Guerra-Lopez: *Wear*, **376–377** (2017), 77. <https://doi.org/10.1016/j.wear.2017.02.043>
- 9) R. J. K. Wood: *Friction, Lubrication, and Wear Technology*, ASM Handbook, Vol. 18, ASM International, Materials Park, (2017), 266.
- 10) K.-H. Zum Gahr: *Tribol. Int.*, **31** (1998), No. 10, 587. [https://doi.org/10.1016/S0301-679X\(98\)00079-6](https://doi.org/10.1016/S0301-679X(98)00079-6)
- 11) I. R. Sare: *Met. Technol.*, **6** (1979), No. 1, 412. <https://doi.org/10.1179/030716979803276228>
- 12) H. Berns, A. Fischer and W. Theisen: *Proc. 5th Int. Conf.*, Vol. 1, Pergamon Press, Beijing, China, (1987), 285.
- 13) W. L. Bradley and M. N. Srinivasan: *Int. Mater. Rev.*, **35** (1990), 129. <https://doi.org/10.1179/095066090790324028>
- 14) Y. Jian, Z. Huang, J. Xing and J. Li: *Wear*, **378–379** (2017), 165. <https://doi.org/10.1016/j.wear.2017.02.042>
- 15) K. M. Ibrahim and M. M. Ibrahim: *J. Metall.*, **2014** (2014), 856408. <https://doi.org/10.1155/2014/856408>
- 16) R. J. Chung, X. Tang, D. Y. Li, B. Hinckley and K. Dolman: *Wear*, **267** (2009), 356. <https://doi.org/10.1016/j.wear.2008.12.061>
- 17) A. Bedolla-Jacuinde, F. Guerra, I. Mejía and U. Vera: *Metals*, **9** (2019), 1321. <https://doi.org/10.3390/met9121321>
- 18) C. G. Oliveira and I. Pinheiro: *Effect of Niobium on Microstructure of High Chromium White Cast Iron*, Cambridge University Press, Cambridge, UK, (2016).
- 19) J. Opapaiboon, M. Supradist Na Ayudhaya, P. Sricharoenchai, S. Inthidech and Y. Matsubara: *J. Met., Mater. Miner.*, **28** (2018), 94. <https://doi.org/10.14456/jmmm.2018.32>
- 20) M. Hashimoto, O. Kubo and Y. Matsubara: *ISIJ Int.*, **44** (2004), 372. <https://doi.org/10.2355/isijinternational.44.372>
- 21) K. Kusumoto, K. Shimizu, X. Yaer, Y. Zang, Y. Ota and J. Ito: *Wear*, **376–377** (2017), 22. <https://doi.org/10.1016/j.wear.2017.01.096>
- 22) Y. Zang, K. Shimizu, K. Kusumoto, H. Hara and C. Higuchi: *Wear*, **376–377** (2017), 452. <https://doi.org/10.1016/j.wear.2016.12.044>
- 23) H. Gasan and F. Erturk: *Metall. Mater. Trans. A*, **44** (2013), 4993. <https://doi.org/10.1007/s11661-013-1851-3>
- 24) J. Wang, Z. Sun, B. Shen, S. Gao, R. Zuo, C. Li and S. Huang: *J. Mater. Eng. Perform.*, **15** (2006), 316. <https://doi.org/10.1361/105994906X108602>
- 25) A. E. Karantalis, A. Lekatou and E. Diavati: *J. Mater. Eng. Perform.*, **18** (2009), 1078. <https://doi.org/10.1007/s11665-009-9353-6>
- 26) G. L. F. Powell and G. Laird II: *J. Mater. Sci.*, **27** (1992), 29. <https://doi.org/10.1007/BF00553833>
- 27) S. Inthidech, A. Chooprajong, P. Sricharoenchai and Y. Matsubara: *Mater. Trans.*, **53** (2012), 1258.
- 28) I. Fordyce, M. Annasamy, S. D. Sun, D. Fabijanic, S. C. Gallo, M. Leary, M. Easton and M. Brandt: *Wear*, **458–459** (2020), 203410. <https://doi.org/10.1016/j.wear.2020.203410>
- 29) J. R. Keough and K. L. Hayrynen: *Cast Iron Science and Technology*, ASM Handbook, Vol. 1A, ASM International, Materials Park, (2017), 275.
- 30) S. K. Yu, N. Sasaguri and Y. Matsubara: *Int. J. Cast Met. Res.*, **11** (1999), 561.
- 31) K. Kishore, U. Kumar, N. Dinesh and M. Adhikary: *J. Fail. Anal. Prev.*, **20** (2020), 249. <https://doi.org/10.1007/s11668-020-00836-7>
- 32) Y. Li, P. Li, K. Wang, H. Li, M. Gong and W. Tong: *Vacuum*, **156** (2018), 59. <https://doi.org/10.1016/j.vacuum.2018.07.013>
- 33) G. Laird, R. Gundlach and K. Röhrig: *Abrasion-Resistant Cast Iron Handbook*, AFS, Schaumburg, (2000), 76.
- 34) K. Kusumoto, K. Shimizu, V. G. Efremenko, H. Hara, M. Shirai, J. Ito, M. Hatate, Y. Gaqi and R. H. Purba: *Wear*, **426–427** (2019), 122. <https://doi.org/10.1016/j.wear.2019.01.108>
- 35) A. Takeuchi and A. Inoue: *Mater. Trans.*, **46** (2005), 2817.
- 36) J. Opapaiboon, M. Supradist Na Ayudhaya, P. Sricharoenchai, S. Inthidech and Y. Matsubara: *Mater. Trans.*, **60** (2019), 346.
- 37) W. Khanitnantharak, M. Hashimoto, K. Shimizu, K. Yamamoto, N. Sasaguri and Y. Matsubara: *AFS Trans.*, **117** (2009), 435.